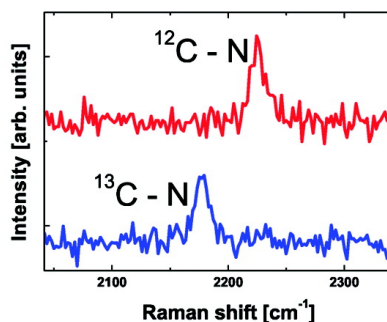
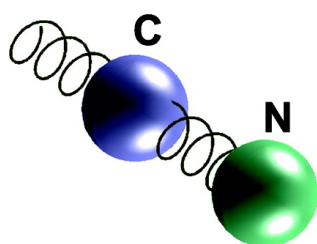


## Evidence of Natural Isotopic Distribution from Single-Molecule SERS

Pablo G. Etchegoin, Eric C. Le Ru, and Matthias Meyer

*J. Am. Chem. Soc.*, **2009**, 131 (7), 2713-2716 • DOI: 10.1021/ja808934d • Publication Date (Web): 23 January 2009

Downloaded from <http://pubs.acs.org> on February 18, 2009



### More About This Article

Additional resources and features associated with this article are available within the HTML version:

- Supporting Information
- Access to high resolution figures
- Links to articles and content related to this article
- Copyright permission to reproduce figures and/or text from this article

[View the Full Text HTML](#)

## Evidence of Natural Isotopic Distribution from Single-Molecule SERS

Pablo G. Etchegoin,\* Eric C. Le Ru,\* and Matthias Meyer\*

*The MacDiarmid Institute for Advanced Materials and Nanotechnology, School of Chemical and Physical Sciences, Victoria University of Wellington, P.O. Box 600, Wellington, New Zealand*

Received November 20, 2008; E-mail: Pablo.Etchegoin@vuw.ac.nz; Eric.LeRu@vuw.ac.nz; kiwimatto@gmail.com

**Abstract:** We report on the observation of the natural isotopic spread of carbon from single-molecule surface-enhanced Raman spectroscopy (SM-SERS). By choosing a dye molecule with a very localized Raman-active vibration in a cyano bond (C≡N triple bond), we observe (in a SERS colloidal liquid) a small fraction of SM-SERS events where the frequency of the cyano mode is softened and in agreement with the effect of substituting  $^{12}\text{C}$  by the next most abundant isotope,  $^{13}\text{C}$ . This example adds another demonstration of single-molecule sensitivity in SERS through isotopic editing, which in this case is done not by artificial isotopic editing but rather by nature itself. It also highlights SERS as a unique spectroscopic tool that is capable of detecting an isotopic change in one atom of a single molecule.

### Introduction

As a spectroscopic technique, single-molecule surface-enhanced Raman scattering (SM-SERS) is now well-established and accepted. A précis of some of its most salient aspects has recently been provided in ref 1. Arguably, one of the most refined and elegant demonstrations of SM-SERS is through the bianalyte SERS technique<sup>2–4</sup> using isotopically edited molecules.<sup>5,6</sup> Isotopic editing is done purposely on specific moieties of standard SERS probes (e.g., rhodamines)<sup>5,6</sup> to obtain molecules that have nominally identical chemical properties but distinguishable Raman features.

Still, the typical atoms that constitute the structure of standard dyes used for SERS have their own natural isotopic spread. Accordingly, we can ask if the reverse logic applies: under SM-SERS conditions, is it possible to discern natural isotopologues? In this paper, we show that in specific cases, the natural isotopic spread of carbon in organic dyes is indeed detectable.

### Background

One of the obvious contributions to the isotopic distribution of organic molecules of interest for SERS is carbon. Despite a relatively small natural isotopic spread between  $^{12}\text{C}$  (98.9%) and  $^{13}\text{C}$  (1.1%),<sup>7</sup> carbon still plays a decisive role in the isotopic spread of organic molecules because of its preponderance with

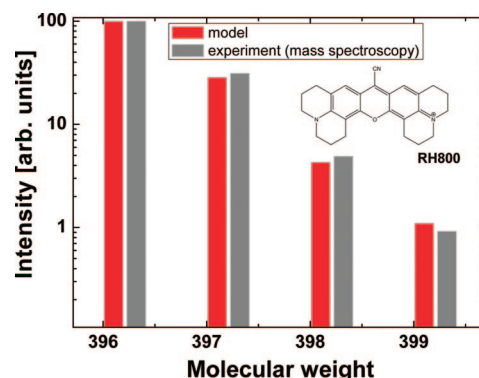


**Figure 1.** Experimental (gray) and calculated (red) abundances of isotopologues of RH800 (inset) produced by the natural isotopic spread of its constituent atoms. The experimental results were obtained by high-resolution mass spectroscopy. Approximately 20% of RH800 molecules have one more unit of mass because of the  $^{12}\text{C} \rightarrow ^{13}\text{C}$  isotopic substitution in the structure (the rest corresponding to other isotopic substitutions). The number of molecules that have the  $^{12}\text{C} \rightarrow ^{13}\text{C}$  substitution at the cyano bond (C≡N) is, however, much smaller (~1%) because there is only *one* such site (i.e., this substitution depends only on the natural isotopic ratio of carbon).

respect to other atomic species. Hydrogen is, of course, also very abundant in typical organic dyes, but this is compensated by its much smaller natural isotopic spread between hydrogen (99.985%) and deuterium (0.015%).<sup>7</sup> Let us study one particular example of a useful SERS probe: rhodamine 800 (RH800). The reason for choosing this particular molecule will become clearer later. The structure of RH800 is shown in the inset of Figure 1; it has the chemical formula  $\text{C}_{26}\text{H}_{26}\text{N}_3\text{O}^+$  and a molar mass of 396.21 g/mol when all of the atoms are in their most abundant (here, their lightest) isotopes. Carbon and hydrogen are the most abundant atoms in the structure. Not only are nitrogen and oxygen a minority, but they also have smaller natural isotopic spreads than carbon does (99.63% for  $^{14}\text{N}$  and 0.37% for  $^{15}\text{N}$ ; 99.75% for  $^{16}\text{O}$ , 0.05% for  $^{17}\text{O}$ , and 0.20% for  $^{18}\text{O}$ ).<sup>7</sup> It is quite clear that having the largest abundance and the widest (relative)

- (1) Etchegoin, P. G.; Le Ru, E. C. *Phys. Chem. Chem. Phys.* **2008**, *10*, 6079–6089.
- (2) Le Ru, E. C.; Meyer, M.; Etchegoin, P. G. *J. Phys. Chem. B* **2006**, *110*, 1944–1948.
- (3) Goulet, P. J. G.; Aroca, R. F. *Anal. Chem.* **2007**, *79*, 2728–2734.
- (4) Sawai, Y.; Takimoto, B.; Nabika, H.; Ajito, K.; Murakoshi, K. *J. Am. Chem. Soc.* **2007**, *129*, 1658–1662.
- (5) Dieringer, J. A.; Lettan, R. B., II; Scheidt, K. A.; Van Duyne, R. P. *J. Am. Chem. Soc.* **2007**, *129*, 16249–16256.
- (6) Blackie, E.; Le Ru, E. C.; Meyer, M.; Timmer, M.; Burkett, B.; Northcote, P.; Etchegoin, P. G. *Phys. Chem. Chem. Phys.* **2008**, *10*, 4147–4153.
- (7) de Laeter, J. R.; Böhlke, J. K.; De Bièvre, P.; Hidaka, H.; Peiser, H. S.; Rosman, K. J. R.; Taylor, P. D. P. *Pure Appl. Chem.* **2003**, *75*, 683–799.

natural isotopic spread (even though it is only  $\sim 1\%$ ) is enough for carbon to play the most predominant role. In fact, the “combinatorics” of isotopic mass distributions are straightforward to calculate and can be compared to direct experimental measurements of the mass distribution of RH800 molecules, a common practice in mass spectroscopy analysis. This is explicitly shown in Figure 1, which was obtained by performing standard high-resolution mass spectroscopy on our sample. It should be noted that mass spectroscopy typically uses large numbers of molecules (i.e., macroscopic samples) to discern these differences.

These natural isotopic changes in mass result, in principle, in slight changes in vibrational frequencies. However, these cannot be resolved in most cases for a variety of reasons, including the following: (i) the natural isotopic spread is very small; (ii) natural isotopic substitutions occur at random places within the molecular structure and not necessarily at places where they can considerably affect the eigenvectors and frequencies of the Raman-active vibrations; and (iii) natural isotopic shifts are in many cases so small that they are hidden within the homogeneous line width of the Raman peaks. In fact, a big fraction of the eigenvectors that produce Raman-active modes in medium-sized or large molecules extend over many atoms,<sup>8</sup> and the perturbation of a small mass change at a certain site is thus relatively minor. From the standard theory of vibrations in molecules, the frequency  $\omega_i$  of a given mode  $i$  in a molecule is related to its reduced mass  $\mu_i$  through the proportionality  $\omega_i \propto \mu_i^{-1/2}$ .<sup>8</sup> The reduced mass can be viewed as an eigenvector-weighted mass average that takes into account the relative participation of different atoms in the collective motion described by a particular eigenvector. A change of mass  $\Delta m_j$  on the  $j$ th atom results in a corresponding change in the frequency  $\omega_i$ , given by  $\Delta\omega_i^j = -[\omega_i/(2\mu_i)]\Delta\mu_i^j$ , where  $\Delta\mu_i^j = (\partial\mu_i/\partial m_j)\Delta m_j$ . In general, this change is small and lies within the intrinsic line width (homogeneous broadening) of the peak.

There are nevertheless exceptions, a family of which is associated with the existence of *localized vibrational modes*, for which  $\partial\mu_i/\partial m_j$  is much larger. RH800 has such a mode. The carbon–nitrogen triple bond (cyano group) in the structure of RH800, highlighted in Figure 2a, is a strong bond that produces a relatively isolated and localized stretch vibration. The cyano group (highlighted in Figure 2b) produces a Raman-active vibration at a frequency  $\omega \approx 2230 \text{ cm}^{-1}$  for the most common isotopic combination,  $^{12}\text{C}\equiv^{14}\text{N}$ . This vibration is fairly localized to the stretch motion of carbon against nitrogen and occurs in the so-called “Raman-silent” region, which is located above the standard fingerprint region ( $\sim 100\text{--}1700 \text{ cm}^{-1}$ ) and below the hydrogen-stretching region ( $\sim 2900\text{--}3100 \text{ cm}^{-1}$ ) for typical organic molecules. The cyano stretch Raman-active mode is shown explicitly in the spectrum in Figure 2c for the specific case of RH800. Only triple bonds produce Raman-active modes in this region. To a very good approximation, it is possible to think of the cyano bond as a “dumbbell” formed by the C and N atoms that is coupled (through a “softer” spring) to the rest of the molecular structure. This is shown explicitly in the inset of Figure 2. As a localized vibration with a high frequency, the C $\equiv$ N stretch is particularly susceptible to isotopic substitution and, in particular, to the most common replacement,  $^{12}\text{C} \rightarrow ^{13}\text{C}$ . The identification is helped by two facts: (i) the shift also occurs in a region where there cannot be any overlap with other Raman-

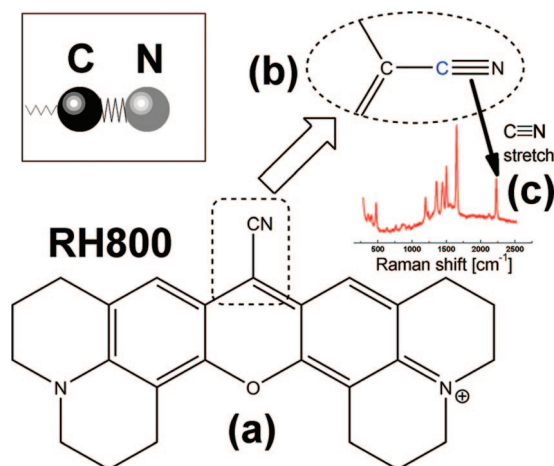


**Figure 2.** (a) Molecular structure of RH800. In (b) we show the immediate environment of the cyano bond (C $\equiv$ N), which forms a localized high-frequency vibration resembling a “dumbbell” (inset). This vibration is Raman-active, as shown in the spectrum in (c), and appears at  $\sim 2230 \text{ cm}^{-1}$  in the so-called “Raman-silent” region (only triple bonds have Raman-active vibrations in this region). As a high frequency *localized* vibration, the cyano stretching mode is particularly susceptible to the isotopic substitution  $^{12}\text{C} \rightarrow ^{13}\text{C}$ , resulting in a frequency softening of the mode by  $\Delta\omega \approx 55 \text{ cm}^{-1}$ .

**Table 1.** C $\equiv$ N Stretch for Different Isotopic Combinations in Cyanobenzene Calculated by DFT<sup>a</sup>

isotopologue	$\omega \text{ (cm}^{-1}\text{)}$	$\Delta\omega \text{ (cm}^{-1}\text{)}$	abundance (%)
$^{12}\text{C}\equiv^{14}\text{N}$	2332	—	98.53
$^{13}\text{C}\equiv^{14}\text{N}$	2277	55	1.1
$^{12}\text{C}\equiv^{15}\text{N}$	2303	29	0.37
$^{13}\text{C}\equiv^{15}\text{N}$	2247	85	0.004

<sup>a</sup> The most likely case observed experimentally is the bond  $^{12}\text{C}\equiv^{14}\text{N}$ , followed by the next most likely ( $\sim 1\%$ ) case of  $^{13}\text{C}\equiv^{14}\text{N}$ , which has a (calculated) frequency softening of  $\Delta\omega \approx 55 \text{ cm}^{-1}$ . See the Supporting Information for more details on the DFT calculations.

active modes, thus facilitating its identification; and (ii) the shift is large enough (because it is proportional to the frequency of the mode) and the peak narrow enough to produce a new peak that cannot be confused as a small shift of the normal case (which could have other origins, such as anharmonic/thermal effects).

For the most abundant case,  $^{12}\text{C}\equiv^{14}\text{N}$ , the reduced mass of the isolated dumbbell changes by  $\Delta\mu \approx 0.28$  for  $^{12}\text{C} \rightarrow ^{13}\text{C}$ . Hence, the predicted change in the cyano frequency ( $\omega_{\text{C}\equiv\text{N}} \approx 2230 \text{ cm}^{-1}$ ) is  $\Delta\omega_{\text{C}\equiv\text{N}} \approx 50 \text{ cm}^{-1}$ . More accurate values that consider the linkage of the dumbbell to the rest of the structure can be obtained by direct calculations using density functional theory (DFT). One advantage of the cyano bond is that, as a localized vibration, it can be modeled with any molecule that resembles the local chemical environment of the bond. For example, we can study the cyano-bond dynamics in RH800 using calculations on the much smaller molecule cyanobenzene ( $\text{C}_6\text{H}_5\text{CN}$ ) with obvious computational advantages. Further details of the calculations are provided in the Supporting Information. A summary of the results is provided in Table 1. A frequency softening of  $\sim 55 \text{ cm}^{-1}$  between the most abundant form of the bond ( $^{12}\text{C}\equiv^{14}\text{N}$ ) and next most abundant one ( $^{13}\text{C}\equiv^{14}\text{N}$ ) is predicted by DFT. Such a shift is much larger than the line width of the corresponding Raman peak and therefore should be easily observable in a small fraction of the SM-SERS spectra.

(8) Le Ru, E. C.; Etchegoin, P. G. *Principles of Surface-Enhanced Raman Spectroscopy and Related Plasmonic Effects*; Elsevier: Amsterdam, 2009.

## Experiment and Discussion

SERS spectra were collected in immersion for RH800 in a silver (citrate-reduced) Lee–Meisel colloid<sup>9</sup> at 10 mM KCl. The experimental conditions were identical to those reported in our recent study of isotopologues of rhodamine in ref 6. A full characterization of the colloidal system we used, including average enhancement factors and SM-SERS properties, has been thoroughly provided in refs 2, 10, and 11. Spectra were obtained with a  $\times 100$  objective indexed-matched to water and the 633 nm line of a HeNe laser. It should be noted that RH800 has an absorption maximum at  $\sim 685$  nm, with the next vibronic peak at  $\sim 626$  nm, almost in resonance with the laser at 633 nm. Therefore, this is formally a surface-enhanced resonant Raman scattering (SERRS) situation. Data were collected using a Jobin-Yvon LabRam spectrometer equipped with a notch filter and a nitrogen-cooled CCD. The dye concentration in the colloidal solution was 10 nM, and 18 000 spectra were taken with an integration time of 0.2 s (with a 1 s dwell time in between spectra to ensure statistical independence). We know from previous characterizations of our system for similar experiments with the bianalyte method<sup>6</sup> that under these conditions, many of the spectra are single-molecule in nature, with a fraction of them having contributions from more than one molecule.

Once the spectra were taken, we needed to find cases where the isotopically modified cyano bond was present. This required looking for a “minority” of cases that did not contribute much to the average signal. We did this using principal component analysis (PCA), as explained in the Supporting Information; however, this is not necessary, and any method should render equivalent results. The big advantage of PCA is that it reduces to a matter of seconds the time required to search for the appropriate spectra, which is a task that becomes very tedious otherwise when 18 000 spectra need to be analyzed.

Figure 3 shows representative spectra of the different cases of interest here. The vast majority of events show only the  $^{12}\text{C}\equiv^{14}\text{N}$  cyano bond Raman peak at  $\sim 2230$   $\text{cm}^{-1}$ . A closer look, however, reveals situations with mixed signals at the corresponding frequencies expected for  $^{12}\text{C}\equiv^{14}\text{N}$  and  $^{13}\text{C}\equiv^{14}\text{N}$ . These are equivalent to the mixed signals that appear in the standard bianalyte method. The experimental frequency softening is  $\sim 56$   $\text{cm}^{-1}$ , in excellent agreement with the DFT predictions (Table 1). We chose three spectra in Figure 3 showing a larger, equivalent, or smaller intensity of the  $^{12}\text{C}\equiv^{14}\text{N}$  peak with respect to that for  $^{13}\text{C}\equiv^{14}\text{N}$ . Finally, we show cases where the signal comes *only* from the isotopically modified cyano bond ( $^{13}\text{C}\equiv^{14}\text{N}$ ). The average SERS spectrum is also shown for direct comparison. It is interesting to note the small feature at  $\sim 2120$   $\text{cm}^{-1}$  with an integrated intensity  $\sim 10$  times less than that of the cyano bond peak. This is assigned to an overtone band and has no relation to the isotopic spread. It does, however, give an idea of how small the  $^{13}\text{C}\equiv^{14}\text{N}$  Raman peak should be in the average signal:  $\sim 10$  times smaller than this  $\sim 2120$   $\text{cm}^{-1}$  overtone band, i.e., clearly undetectable in the average spectrum under the present conditions. This is in stark contrast with the SM-SERS spectra, where the  $^{13}\text{C}\equiv^{14}\text{N}$  cyano bond signal can completely dominate the spectra. The single-molecule nature of the signals here enables us to access

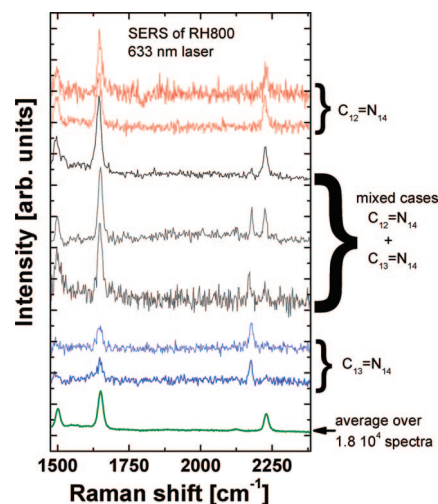


**Figure 3.** SERS spectra of RH800, showing from top to bottom: (i) Normal spectroscopic feature of the Raman mode of the  $^{12}\text{C}\equiv^{14}\text{N}$  cyano bond at  $\sim 2230$   $\text{cm}^{-1}$  (top two spectra, red). (ii) Mixed cases (next three spectra, black) where both the  $^{12}\text{C}\equiv^{14}\text{N}$  and  $^{13}\text{C}\equiv^{14}\text{N}$  cyano bonds can be seen. These mixed spectra appear in the standard bianalyte SERS method, and here we show cases with larger, equivalent, and smaller relative intensities of one peak with respect to the other. (iii) SM-SERS events for the  $^{13}\text{C}\equiv^{14}\text{N}$  cyano bond (next two spectra, blue). (iv) Average spectrum (bottom, green) for the 18 000 obtained spectra. It should be noted that the number of cases where the  $^{13}\text{C}\equiv^{14}\text{N}$  cyano bond signal is observed is very small, as evidenced by the negligible effect on the average spectrum. We show the spectra in a range that includes the  $\sim 1650$   $\text{cm}^{-1}$  mode of RH800, which remains unchanged in all cases (as expected), together with all the other modes in the fingerprint region at lower energies.

information, such as the isotope-induced shift, that is clearly washed out in the ensemble average. It is worth noting that the  $^{12}\text{C}/^{13}\text{C}$  isotopic content ratio cannot be determined very accurately by counting the number of cases where the isotopically shifted peak appears, because of the sparse nature of the statistics under single-molecule conditions and the fact that most of the spectra show no signal at all (with an arbitrary criterion based on a signal-to-noise ratio). Our statistics is compatible with the isotopic content of  $^{13}\text{C}$ , but an accurate number cannot be gained from it. In fact, the most reliable determination of the isotopic content is *not* through the counting of events in the statistics but rather through the average spectrum. This is precisely the advantage of determining (through single-molecule events) where the isotopically shifted peak should be. The fact that one can identify exactly where the peak should be can allow its subsequent quantification, and this is then a new degree of freedom for labeling peaks (added by SM-SERS spectroscopy) that would not exist otherwise.

## Conclusion

The results of this work indirectly provide another demonstration of SM-SERS sensitivity in addition to the ones already known.<sup>1,12,13</sup> However, aside from this, the main claim here is one step beyond another demonstration of SM-SERS sensitivity. We have indeed shown a specific example of how SM-SERS can be used as tool for the observation of weak spectroscopic features that are otherwise washed out in ensemble-averaged spectra. Other types of spectroscopy (such as fluorescence)

(9) Lee, P. C.; Meisel, D. *J. Phys. Chem.* **1982**, *86*, 3391–3395.  
 (10) Meyer, M.; Le Ru, E. C.; Etchegoin, P. G. *J. Phys. Chem. B* **2006**, *110*, 6040–6047.  
 (11) Le Ru, E. C.; Blackie, E.; Meyer, M.; Etchegoin, P. G. *J. Phys. Chem. C* **2007**, *111*, 13794–13803.

(12) Pieczonka, N. P. W.; Aroca, R. F. *ChemPhysChem* **2005**, *6*, 2473–2484.  
 (13) Steidner, J.; Pettinger, B. *Phys. Rev. Lett.* **2008**, *100*, 236101.

would be completely insensitive to a change of one unit in the isotopic mass of *one* atom, even if single-molecule sensitivity is achieved. We believe the observation of naturally occurring single-molecule isotopic fluctuations in SERS is a pleasing demonstration of the consistency of SM-SERS phenomena in revealing subtle aspects of molecular spectroscopy that cannot be observed otherwise. The spectra in Figure 3 effectively show examples of single-molecule Raman spectra of molecules that differ from the others by *one unit* of atomic mass in *one* atom. Finally, it is also worth pointing out that the observation of a natural isotopic spread with SM-SERS is not necessarily restricted to triple bonds. Options with chlorine-containing dyes could be particularly interesting to explore, for the natural

isotopic spread of chlorine can produce a much more balanced list of naturally occurring isotopologues.

**Acknowledgment.** We are indebted to Sean Buchanan for help with the measurements. P.G.E. and E.C.L.R. acknowledge partial support from the Royal Society of New Zealand (RSNZ) through a Marsden Grant.

**Supporting Information Available:** Details concerning the DFT calculations of vibrational frequencies of the cyano bond and the PCA of the SERS spectra to isolate the isotopically modified cases. This material is available free of charge via the Internet at <http://pubs.acs.org>.

JA808934D